



Anchoring conductive polymeric monomers on single-walled carbon nanotubes: towards covalently linked nanocomposites

Naiane Naidek, Kai Huang, George Bepete, Maria Luiza M. Rocco, Alain Pénicaud, Aldo Zarbin, Elisa Orth

► To cite this version:

Naiane Naidek, Kai Huang, George Bepete, Maria Luiza M. Rocco, Alain Pénicaud, et al.. Anchoring conductive polymeric monomers on single-walled carbon nanotubes: towards covalently linked nanocomposites. *New Journal of Chemistry*, 2019, 43 (26), pp.10482-10490. 10.1039/c9nj01817d . hal-02415523

HAL Id: hal-02415523

<https://hal.science/hal-02415523>

Submitted on 27 Nov 2020

HAL is a multi-disciplinary open access archive for the deposit and dissemination of scientific research documents, whether they are published or not. The documents may come from teaching and research institutions in France or abroad, or from public or private research centers.

L'archive ouverte pluridisciplinaire **HAL**, est destinée au dépôt et à la diffusion de documents scientifiques de niveau recherche, publiés ou non, émanant des établissements d'enseignement et de recherche français ou étrangers, des laboratoires publics ou privés.

Anchoring conducting polymeric monomers on single-walled-carbon nanotubides: towards covalently linked nanocomposites

Naiane Naidek¹, Kai Huang², George Bepete², Maria Luiza M. Rocco³, Alain Pénicaud², Aldo J. G. Zarbin¹, Elisa S. Orth^{1*}

¹Department of Chemistry, Universidade Federal do Parana (UFPR), CP 19081, CEP 81531-990, Curitiba, PR, Brazil

²Université Bordeaux 1, CNRS Centre de Recherche Paul Pascal, 115 avenue du dr. A. Schweitzer, 33600 Pessac, France.

³Institute of Chemistry, Federal University of Rio de Janeiro (UFRJ), 21.941-909, Rio de Janeiro, RJ, Brazil

* Corresponding author: Tel: +55 41-33613184; Fax: +55 41-33613186; E-mail: elisaorth@ufpr.br

Abstract:

The functionalization of carbon nanotubes (CNTs) has long been a challenge, due to the low reactivity of CNTs. Herein we present a novel approach to functionalize CNT with three different monomers of conductive polymers, all by means of a covalent bond directly on the carbon surface. A polymeric nanocomposite covalently linked, derived from polypyrrole (Ppy) was also obtained. Firstly, highly reactive negatively charged single wall CNTs (SWCNT) salts were functionalized with monomers of conductive polymers: 3-Bromothiophene, 3-Acetylthiophene and 1-(2-Bromoethyl)-1H-pyrrole, leading to three CNT-functionalized materials. After the functionalization, a “grafted from” approach was used to polymerize the pyrrole-derived CNT and obtain a final, covalently linked, polymeric nanocomposite of SWCNTs/Ppy. All samples were characterized by X-ray photoelectron spectroscopy, thermogravimetric analysis, scanning electron microscopy, infrared and Raman spectroscopy, which confirmed the functionalization and the nanocomposite polymerization. Overall, the results evidence the efficiency of the covalent functionalization directly on the skeleton of the CNTs, followed by the polymerization and formation of a novel covalently linked nanocomposite of Ppy and SWCNTs. These materials are particularly interesting since their synergistic effect can benefit future optimal applications such as supercapacitors and artificial muscles.

* Corresponding author: Tel: +55 41-33613184; Fax: +55 41-33613186; E-mail:

elisaorth@ufpr.br

Keywords: covalent functionalization, nanocomposites, carbon nanotubes, conducting polymers, polypyrrole.

* Corresponding author: Tel: +55 41-33613184; Fax: +55 41-33613186; E-mail:
elisaorth@ufpr.br

1. Introduction

Carbon nanotubes (CNT) comprise a very interesting class of materials with unique morphologies and a structure providing extraordinary mechanical properties with a high Young modulus (around 1 TPa) and tensile strength (up to 300 GPa), extraordinary electrical and thermal properties. Promising applications are foreseen for CNTs in several areas such as electronics, medicine and automotive among others.[1] However, their poor dispersibility in any solvents constitutes a limitation towards further applications. The preparation of modified CNT containing attached molecules allows to overcome the lack of CNT dispersibility. Several compounds may interact with CNT by different interactions and the main approaches to modify the CNTs are based on the (i) covalent and non-covalent functionalization of the surface of the CNTs and on (ii) filling of the empty cavity of the CNT with molecules or metal oxides.[2-5]

Seeking for new and optimized properties, CNT surface functionalization is a perfect way to overcome the drawbacks of the lack of dispersibility and maximize CNT potential applications. The non-covalent functionalization of CNTs is an interesting approach, and can occur by the adsorption or wrapping of functional molecules, surfactants or polymers through van der Waals interactions, π - π stacking and hydrogen bonding, among others.[3, 6, 7] However, these are weak interactions and the groups are not effectively linked to the CNT surface, becoming easily susceptible to leaching, which can sometimes compromise the application. Another approach for functionalization is the covalent bonding onto the CNT surface that can be realized by several organic reactions such as halogenation, hydrogenation, cycloaddition, radical additions, electrophilic addition, among others. Indeed, these reactions allow the inclusion of organic molecules by a covalent bond on the CNT surface avoiding leaching. They also allow the additional insertion of different functional groups or

polymers on functionalized CNTs. With hexagonal rings of carbon sp^2 hybridization, [8] the addition of molecules on the CNTs surface alters the extended π system due the formation of sp^3 carbons, thus changing their electronic properties that could open the field of new applications possibilities [9].

Covalent functionalization is limited by CNT surface reactivity, which is close to the reactivity of alkenes. The functionalization reactions usually require high temperatures (60° up to 500°C) and several reactions steps. Chemical functionalization allows to add functional groups such as oxygenated, amino or alkane groups directly on the CNTs surface. Oxygenated groups such as carboxylic, hydroxyl and epoxy are also promising targets to carry out site-directed functionalization, for example leading to ester and amide linkage or epoxy opening. Moreover, CNT can be functionalized with monomers that can further be polymerized, forming covalently attached polymeric nanocomposites derived from CNTs, yielding synergistic effects between CNTs and polymers [1, 10].

Covalent and non-covalent surface functionalization have shown great results in several applications[11-15]. However, approaches for covalent functionalization usually require several steps or high temperature reactions, especially for obtaining polymeric nanocomposites. Some examples are summarized in Figure 1. One of the simplest functionalization reactions is the halogenation of CNT, which may happen by the fluorination of CNTs (Figure 1A). The reaction takes part with fluorinated compounds from room to high temperatures (500°C) and can be extended to chlorine and bromine.[3, 16, 17] Also, CNTs have been subjected to glow discharge and atomic hydrogen providing hydrogenated CNT, shown in Figure 1B.[18] In another study, CNTs were functionalized with alkylhalides (Br, I and Cl) through an electrophilic addition (Figure 1C), under microwave conditions.[19]

In fact, covalent functionalization can provide new properties, and the efficiency of covalent functionalization was demonstrated by Polyakov *et al* through a covalent link between single wall CNT (SWCNT) and a molecule containing zinc and phthalocyanine (ZnPc, Figure 1D). The nanocomposite was used as sensor, detecting low concentrations of ammonia, CO₂ and other gas.[20, 21] Both covalent and non-covalent functionalization showed great improvement on gas response sensing, and the covalently anchored nanocomposite shows a higher sensor response than the non-covalent nanocomposite. CNT functionalization through a free radical addition of a sulfur derivative species has also been reported [22] in two steps: free radical functionalization with sulfur powder and UV irradiation, followed by the reduction with NaBH₄.(Figure 1E). The obtained CNT-SH was able to be further functionalized with epoxy, alkene and thiol compounds. In another approach Yao *et al*[23] have reported a strategy to obtain polymeric nanocomposites which involves the functionalization of CNTs with cycloalkanes (in acetone, trimethylamine (TEA), dimethylfuran (DMF) and dimethylsulfoxide (DMSO)). For the functionalization, the first step requires a 1,3-dipolar cycloaddition followed by an esterification with 2-bromoisobutyryl bromide (Figure 1F). After the second reaction, the functionalized CNT was polymerized with methyl methacrylate forming the polymerized nanocomposite. Covalently linked polymeric nanocomposites of CNT also may occur by 3 steps as shown in (Figure 1G), (i) formation of the acid-functionalized MWCNT (MWCNT-COOH) followed by (ii) reaction with SOCl₂ and Br derivatives and (iii) reaction based on the reversible addition fragmentation chain-transfer (RAFT polymerization) with the RAFT agent PhC(S)SMgBr.[24] The resulting material was polymerized with the assistance of 2,2'-Azobis(2-methylpropionitrile) (AIBN).

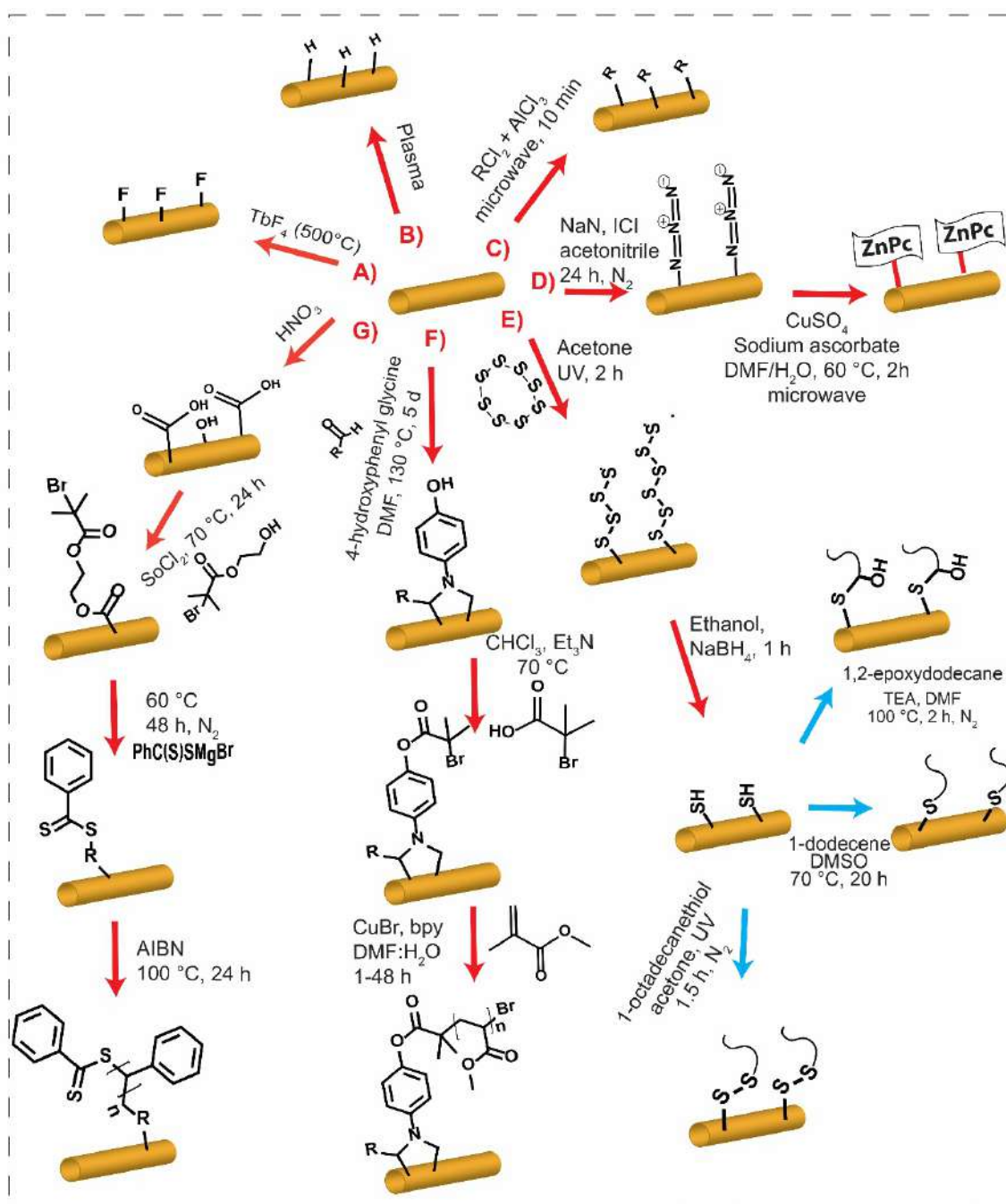


Figure 1. Summary of some reported functionalization of CNTs and formation of nanocomposites, adapted from references.[17, 19-24]

Herein, we propose a more straightforward method for functionalizing CNT with monomers and further obtaining a polymeric nanocomposite covalently linked. Specifically, we targeted reduced nanotube salts, which are negatively charged and

highly reactive in reductive functionalization. Previous reports by Voiry *et al* have shown a stoichiometric control of SWCNT functionalization using reduced nanotube salts with 1-bromo-decanoic acid and 4-(5-bromopentyloxy)-40-cyanobiphenyl while Hof *et al* studied the functionalization of oxygenated SWCNT with thiophene coupled derivatives through ester linkages [9, 25-30]. Moreover, this functionalization directly on the carbon backbone has not been reported yet with monomers of conducting polymers, to the best of our knowledge. Herein we report a novel SWCNT-derived nanocomposite with polypyrrole (Ppy) covalently linked by a “grafted from” approach for the growth of the polymers, Figure 2. Firstly, we anchored the monomers 3-bromothiophene (BTI), 3-acetylthiophene (BATI) and 1-(2-bromoethyl)-1H-pyrrole (BPI) on the CNT surface, using reductive functionalization, with the functionalization directly on the surface of SWCNT. This gave three materials, namely: SWCNT-BTI, SWCNT-BATI and SWCNT-BPI, respectively. Further, as a proof of concept, the sample functionalized with BPI was polymerized using FeCl_3 in order to obtain a covalently linked nanocomposite of SWCNT and Ppy, giving Poly-SWCNT-BPI. The samples were fully characterized by X-Ray photoelectron spectroscopy (XPS), scanning electron microscopy (SEM), infrared (FTIR) and Raman spectroscopy, and thermogravimetric analysis (TGA). Overall, we have successfully obtained the proposed functionalized materials, which are promising candidates for a wide spectrum of applications.

2. Experimental details

The reactants employed in the synthesis of the nanocomposites were BTI (97%), BPI (97%) and BATI (97%), dimethyl sulfoxide (DMSO) (97%), $\text{FeCl}_3 \cdot 6\text{H}_2\text{O}$ ($\geq 98\%$)

obtained from Sigma-Aldrich and pyrrole (99%) from Acros organics. The reduced nanotubes salt was obtained from a SWCNT (CoMoCAT®) using a previously described method, using potassium. [2, 9]

2.1 Preparation of SWCNT salt

The potassium salt of SWCNTs was prepared by reacting potassium with SWCNT powder on a hot plate, under an inert argon-filled glovebox environment as has been reported before for nanotubes and for graphite intercalation.[25, 31, 32] Stoichiometry was chosen as KC_{10} to have a sufficiently high functionalization upon later exposure to the monomers BTI, BATI and BPI.[33] In a typical reaction, 50 mg of freshly cut potassium metal was added to a 20 mL glass vial containing a 150 mg SWCNT sample. The mixture of potassium and SWCNT sample contained in a glass vial was heated on a hot plate at 180 °C with continuous mixing for 10 min using a stainless-steel spatula. The vial was left on the hot plate, and the mixture was mixed with the stainless-steel spatula at every 10 min interval for 1 h and then every 30 min for 4 h. The product was allowed to cool to room temperature, and the vial was tightly capped for later use.

2.2 Functionalization of SWCNT salt

To avoid oxidation of SWCNT salt, the entire procedure was carried out in a glovebox under inert atmosphere.[9, 34] 100 mg of SWCNT salt and 50 mL of ultra dry DMSO (dried through an Inert™ column directly delivering dry solvent inside the box) were left stirring overnight in a round-bottom flask and centrifuged 2 times, at 4000 rpm for 30 min. The undissolved material was separated from the solution. The covalent functionalization was carried out with monomers: BATI, 0.73 g (3.55 mmol), BTI, 400 µL (4.3 mmol) and BPI, 500 µL (4.1 mmol) solubilized in 2 mL ultra dry DMSO. The

monomers were separately added at once to 30 mL of SWCNT salt solution and left to stir for 24 h. A precipitate was obtained, indicative of functionalization. The suspensions of reacted SWCNTs were exposed to air, out of the glovebox, washed with HCl (2 mol L⁻¹) deionized water and then with ethanol, by centrifugation. The final solids were dried in an oven under vacuum at 50 °C for 19 h and the samples were named SWCNT-BATI, SWCNT-BTI and SWCNT-BPI.

2.3 Chemical polymerization of SWCNT-BPI

Polymerization of the covalently functionalized nanotube (SWCNT-BPI) was achieved by the addition of 3.5 µL of a pyrrole monomer solution (0.05 mmol) in a round-bottom flask containing 4 mL (0.4 mg.mL⁻¹) of SWCNT-BPI in aqueous solution. The dispersion was kept stirring while 5 mL of the oxidizing agent FeCl₃.6H₂O (0.25 mol.L⁻¹, 1.25 mmol) in aqueous solution was added slowly. The dispersion was then stirred at room temperature for 6 hours. The final solid Poly-SWCNT-BPI, was separated by vacuum filtration, washed with distilled water and dried in oven at 50 °C.

For comparison purposes, the synthesis of bare Ppy was carried out under the same polymerization conditions described above, however without the presence of SWCNT-BPI. Also, an oxidized sample, namely SWCNT-Ox was synthesized by exposing the reduced carbon nanotubes to air, just the same way as the SWCNT-BPI was exposed to air after synthesis. Finally, a non-covalently linked nanocomposite between SWCNT-Ox and Ppy was synthesized in order to compare. A procedure similar to that described for obtaining the Poly-SWCNT-BPI was used, albeit using SWCNT-Ox instead of SWCNT-BPI, as initial precursor. The non-covalent nanocomposite was named SWCNT-Ox-Ppy. After synthesis, all samples were separated by vacuum

filtration, washed with distilled water and dried in an oven at 50 °C. Figure 2 presents an overall summary of all samples synthesized.

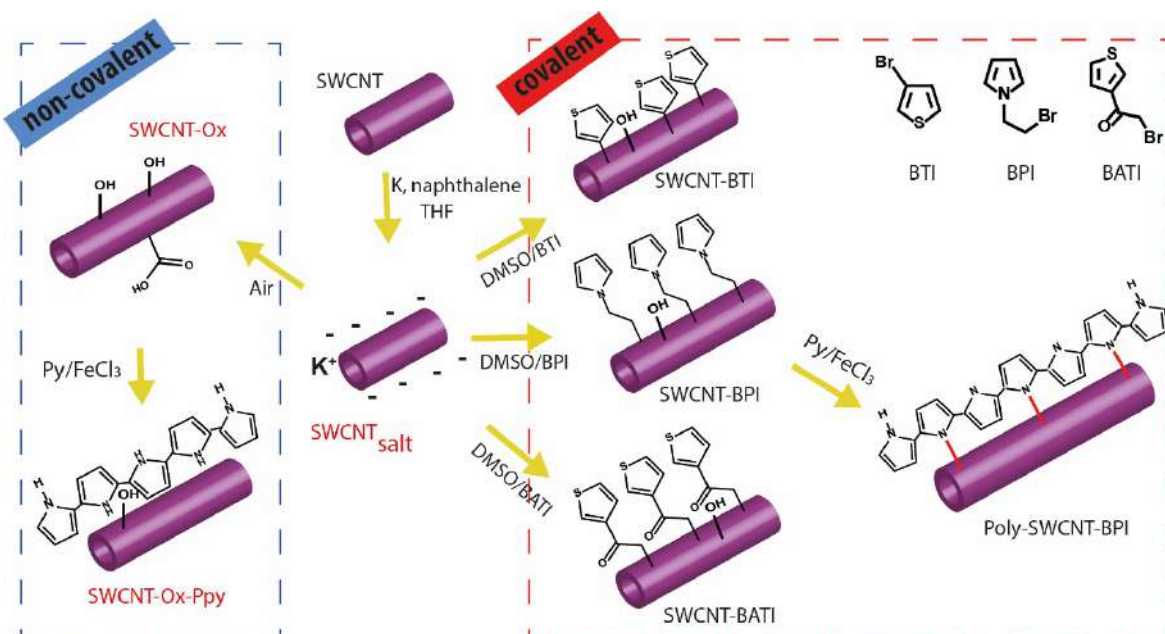


Figure 1. Summary of the functionalization scheme

2.4 Characterization of the samples

XPS analyses were performed on a Thermo Scientific ESCALAB 250Xi spectrometer using monochromatized Al K α ($h\nu = 1486.6$ eV) excitation energy with an X-ray spot size of 650 μm . The high resolution core level and survey spectra were obtained with a constant pass energy of 25 eV and 100 eV, respectively. Raman spectra were acquired with a Renishaw spectrophotometer with 225 μW laser intensity with 632.8 nm excitation laser. The calculation of the ratio I_D/I_G was performed using the average of the areas of the deconvoluted D and G bands of 20 spectra of each sample. The FTIR spectra were obtained in a spectrophotometer Bomem with 64 accumulations using KBr pellets. SEM images were acquired on a Tescan SEM, by deposition of the powder dispersed in isopropanol on a silicon substrate. TGA analyses were performed

on a TA instrument SDT Q600 model with a heating rate of 5 °C.min⁻¹ varying the temperature from ambient to 1000 ° C, using synthetic air atmosphere.

3. Results and discussion

The functionalization targeted herein lead to various samples that were thoroughly investigated by several techniques. It is important to note that the first indication of the successful functionalization is the precipitation during the reaction. All samples (reduced SWCNT salts and functionalized SWCNT salts) were handled under inert atmosphere (glovebox) during the synthesis. At the end of the synthesis the samples were exposed to air (outside the glovebox) and they oxidized as a consequence of the high reactivity of the SWCNT salts [9]. Note that even after functionalization, it has been reported that some unreacted charges remain on the CNTs, leading to hydrogenation and hydroxylation.[25] Hence, along with raw SWCNTs, the analogous oxidized SWCNT-Ox will be used for comparison throughout the characterization. Functionalization of the SWCNTs with BPI, BTI and BATI was first confirmed by the XPS measurements presented in **Erreur ! Source du renvoi introuvable.**3. XPS survey spectra show two main peaks, at 285.0 eV for C1s and at 532.0 eV for O1s [35]. One indication of functionalization of CNT with BPI, BTI and BATI is the low amount of oxygen presented in the XPS spectra of the functionalized samples. Furthermore, for the SWCNT-BPI spectrum, a new peak is observed at 400.0 eV which refers to the N1s core level and thus to the nitrogen bond [35]. The quantities of C, N and O for the SWCNT-BATI, SWCNT-BTI and SWCNT-BPI samples are shown in Table 1. The presence of 2.43% of N and the decrease of O (down to 5.39%) for SWCNT-BPI confirms the functionalization of the CNT.

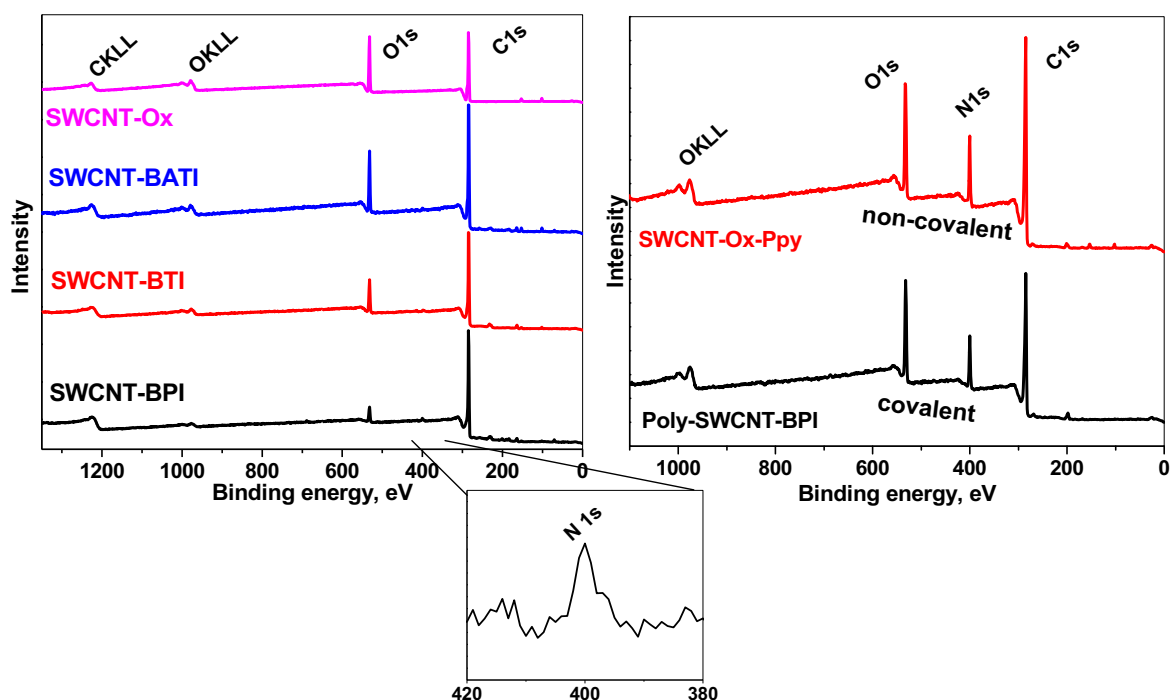


Figure 3. XPS survey spectra of SWCNT-Ox, SWCNT-BPI, SWCNT-BATI, SWCNT-BTI and the covalently and non-covalently linked nanocomposites.

Regarding the XPS survey spectra of the nanocomposites (Figure 3), C 1s, N 1s, O 1s and Cl 2p core level peaks are present in the spectra of both covalent and non-covalently linked polymerized nanocomposites. Indeed, the quantity of C, N, O and Cl (Table 1) are very similar for both nanocomposites. High resolution N1s core level peaks in the spectra of the polymerized nanocomposites, Poly-SWCNT-BPI (covalent) and SWCNT-Ox-Ppy (non-covalent) agree with the presence of Ppy and the nanocomposite formation, as will be discussed in the following.

Table 1. Surface chemical composition of the functionalized and polymerized nanocomposites, atomic percentage obtained by XPS.







		Sample	C 1s	N 1s	O 1s	S 2p	Cl 2p	Si 2p
covalent		SWCNT-Ox (%)	75.20	0	21.45	0	0	3.35
		SWCNT-BPI (%)	88.74	2.43	5.39	2.00	0	0.88
		SWCNT-BATI (%)	80.78	0	15.12	1.70	0	2.40
		SWCNT-BTI (%)	83.18	0.91	11.64	1.95	0	1.59
		Poly-SWCNT-BPI (%)	69.27	11.80	17.18	0	1.59	0
non-covalent		SWCNT-Ox-Ppy (%)	70.84	11.16	14.80	0	1.75	1.60

Figure 4 shows the deconvolution of the C1s spectra of the samples SWCNT-Ox, SWCNT-BATI, SWCNT-BPI and SWCNT-BTI. For all samples, the main peak presented at 284.8 eV corresponds to C=C sp^2 carbon from the CNT structure. The peak at 286.6 eV can be related to C-O, the peak at 287.2 eV to C=O, 291.5 eV to the $\pi-\pi^*$ shake-up feature [36], and the peak at 288.3 eV is due to O-C=O [37, 38]. For SWCNT-BPI, SWCNT-BTI and SWCNT-BATI samples, the peaks at 285.5 and 285.6 eV are attributed to C-S and C-N contributions, respectively [39, 40]. Furthermore, deconvolution of the N1s XPS spectrum of the SWCNT-BPI sample (Figure 4) shows a main peak at 400.5 eV attributed to neutral -NH- while the feature at lower energy (398.4 eV) can be related to a defect structure such as imine-like nitrogen =N- [41]. The peak present at approximately 396 eV is related to the catalyst (Mo) of the SWCNT. In

short, C1s and N1s XPS spectra of the functionalized samples indicate that the monomers are covalently bonded on the SWCNT surface.

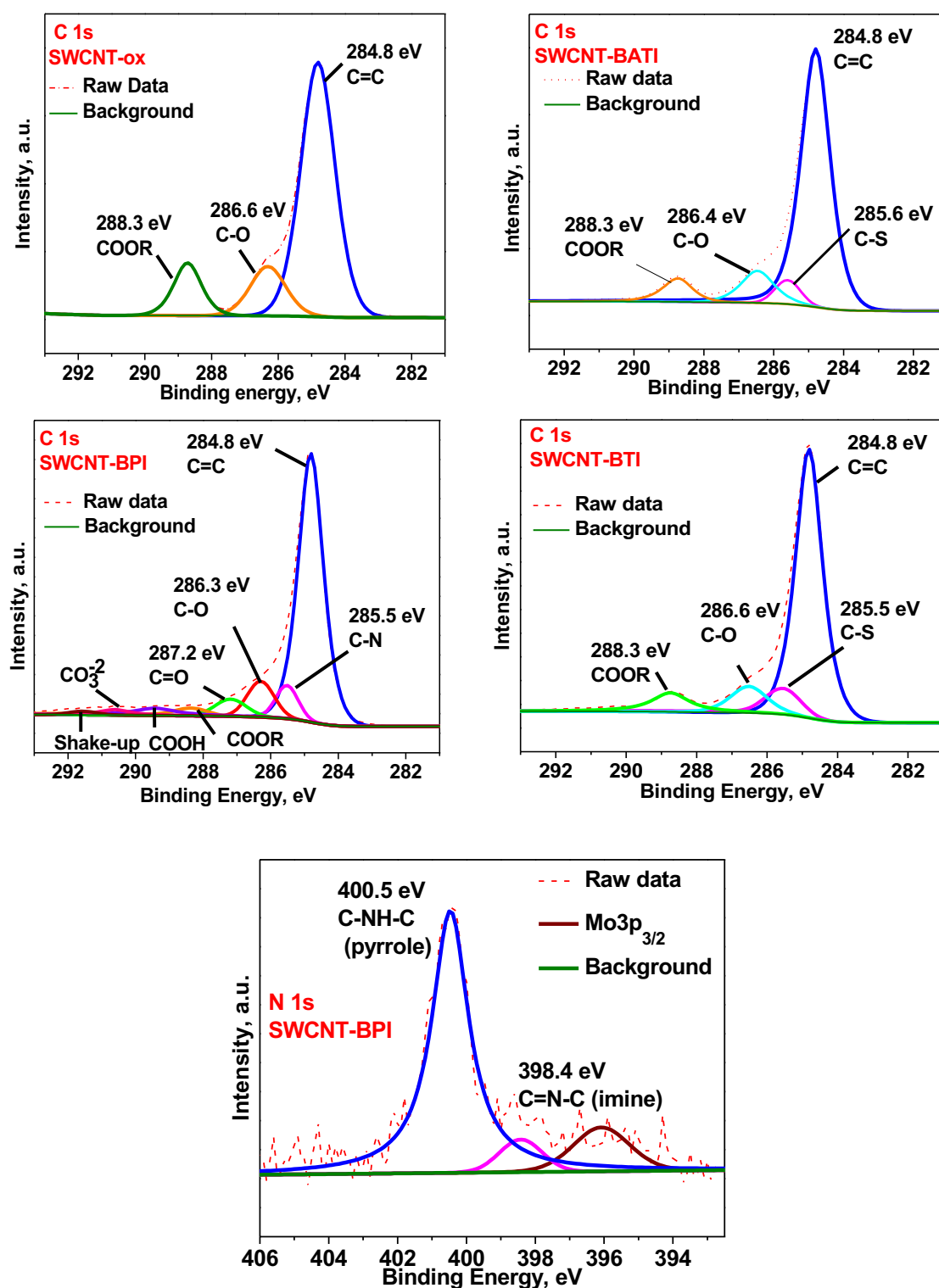


Figure 4. High-resolution C1s XPS spectra of SWCNT-Ox, SWCNT-BATI, SWCNT-BPI and SWCNT-BTI and high-resolution N1s XPS of SWCNT-BPI.

For the covalently and non-covalently linked nanocomposites (Poly-SWCNT-BPI and SWCNT-Ox-Ppy), the C1s high resolution spectra are presented in Figure 5. The peak assignments are very similar to the C1s high resolution spectra of SWCNT-BPI.[37, 38] Regarding the N1s spectra, they were deconvoluted using three Gaussian/Lorentzian peaks: the major peak centered at 400.0 eV is related to the amine-like structure (-NH-) whereas the peak >401 eV is attributed to the positively charged nitrogen atoms (-N⁺) of the Ppy, evidencing its oxidized species, and the peak at 398.1 eV is assigned to the imine-like structure of nitrogen species (=N-) [42, 43]. The obtained results evidence the formation of the nanocomposites and the oxidized form of the polymer due to the presence of charged nitrogen atoms.

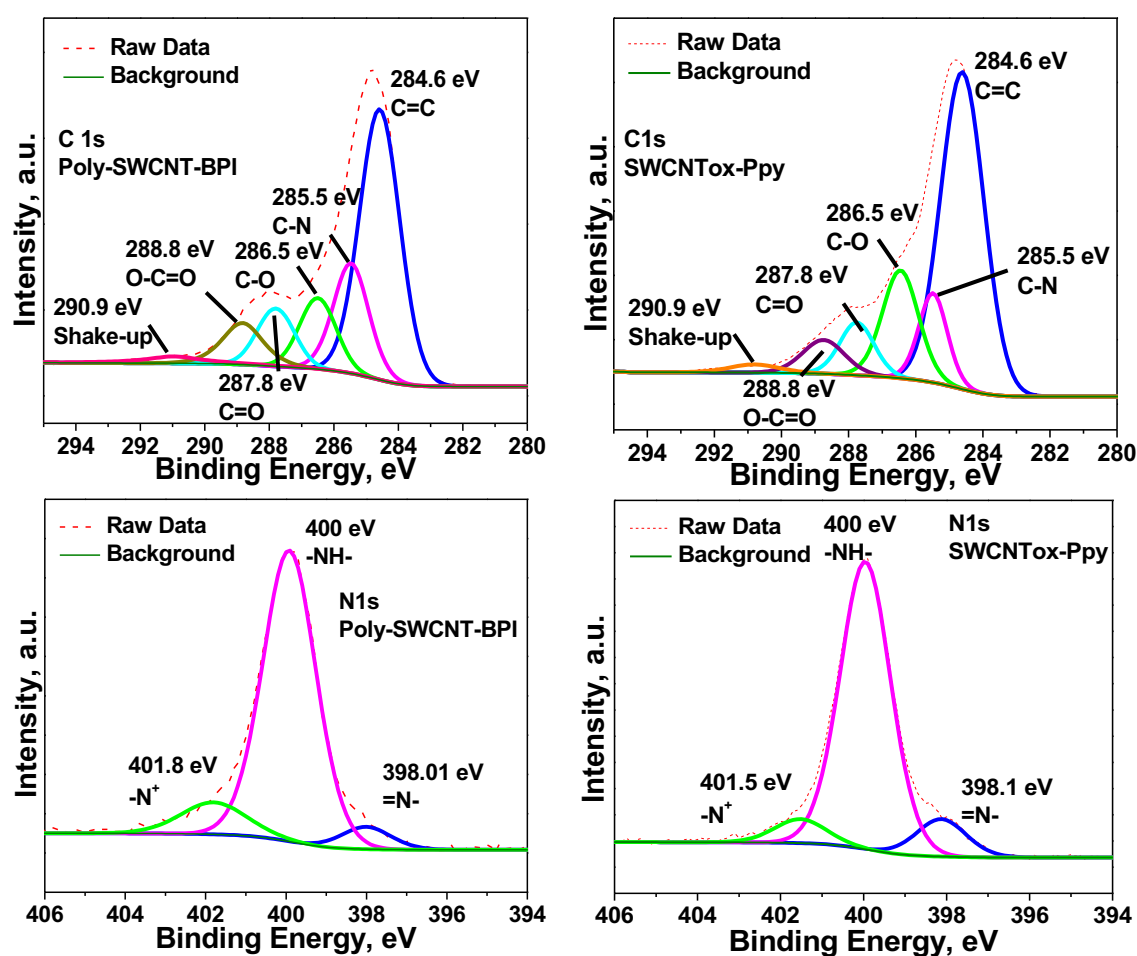


Figure 5. High-resolution C1s and N1s XPS spectra of Poly-SWCNT-BPI and SWCNT-Ox-Ppy.

In order to further characterize the carbon-like structure, the Raman spectra is presented in Figure 6 and shows features providing general information about the CNT. The peaks in the low frequency range below 400 cm^{-1} are known as the radial breathing modes (RBM) of the SWCNT. At higher frequencies, the high intensity peak at 1580 cm^{-1} (G^+ -band) and the low intensity peak at 1532 cm^{-1} (G^- -band) are the two main components of the G-band feature for SWCNT. The first one related to the longitudinal optical mode whereas the latter is related to the transversal optical mode. [44]

Raman bands intrinsic to the functionalized groups were not observed on the Raman spectra of SWCNT-BPI, SWCNT-BATI and SWCNT-BTI, which may be associated to a low degree of functionalization. Even for significant degrees of functionalization ($\sim 30\%$ of the carboxylic acid converted to amides in the case of graphene oxide)[45] no bands associated to the anchored moieties are usually observed due to the characteristic intense bands of the resonant carbon nanomaterials, which dominate the spectra. However, nanotube surface modifications may be evaluated by the D/G ratio. The band at 1300 cm^{-1} (D-band) is related to defects of the sp^2 structure.[44] The ratio of the intensity of the D vs G bands (obtained from the area of the deconvoluted bands) is used to estimate the functionalization degree of carbon nanotubes and higher I_D/I_G values is attributed to greater functionalization.[9, 25] Indeed, the calculated I_D/I_G relation of the samples shows an increase as follows: SWCNT<SWCNT-Ox<SWCNT-BTI<SWCNT-BATI<SWCNT-BPI (Figure 6), indicating a higher degree of defects at the surface of the functionalized materials. As anticipated by XPS, this may be associated with the presence of the BTI, BATI and BPI functional groups onto the surface of SWCNT [9]. The deconvoluted spectra are shown on SI.

Raman spectroscopy of the polymeric Poly-SWCNT-BPI and SWCNT-Ox-Ppy (Figure 6) was used to identify the polymer formation on the nanocomposites covalently and non-covalently linked. New bands are observed in the spectra which are a clear indication of the presence of Ppy. The bands at 926 and 1044 cm^{-1} are correlated to the C-H out-of-plane and the CH stretching of neutral species of Ppy, respectively, [46] whereas the band at ca 1340 cm^{-1} is derived from a superposition of the Ppy bands in the nanocomposite with the SWCT bands. The Ppy spectrum has already been reported in the literature[46, 47] [48] and Table 2 summarizes the main bands of Ppy. The Raman features of SWCNT are still present in these spectra; meanwhile the G and D-band are overlapped by the Ppy Raman bands, making impracticable the I_D/I_G analysis of the nanocomposites. However, the 2D (also called G') band is still visible and not overlapped in the Poly-SWCNT-BPI and SWCNT-Ox-Ppy.

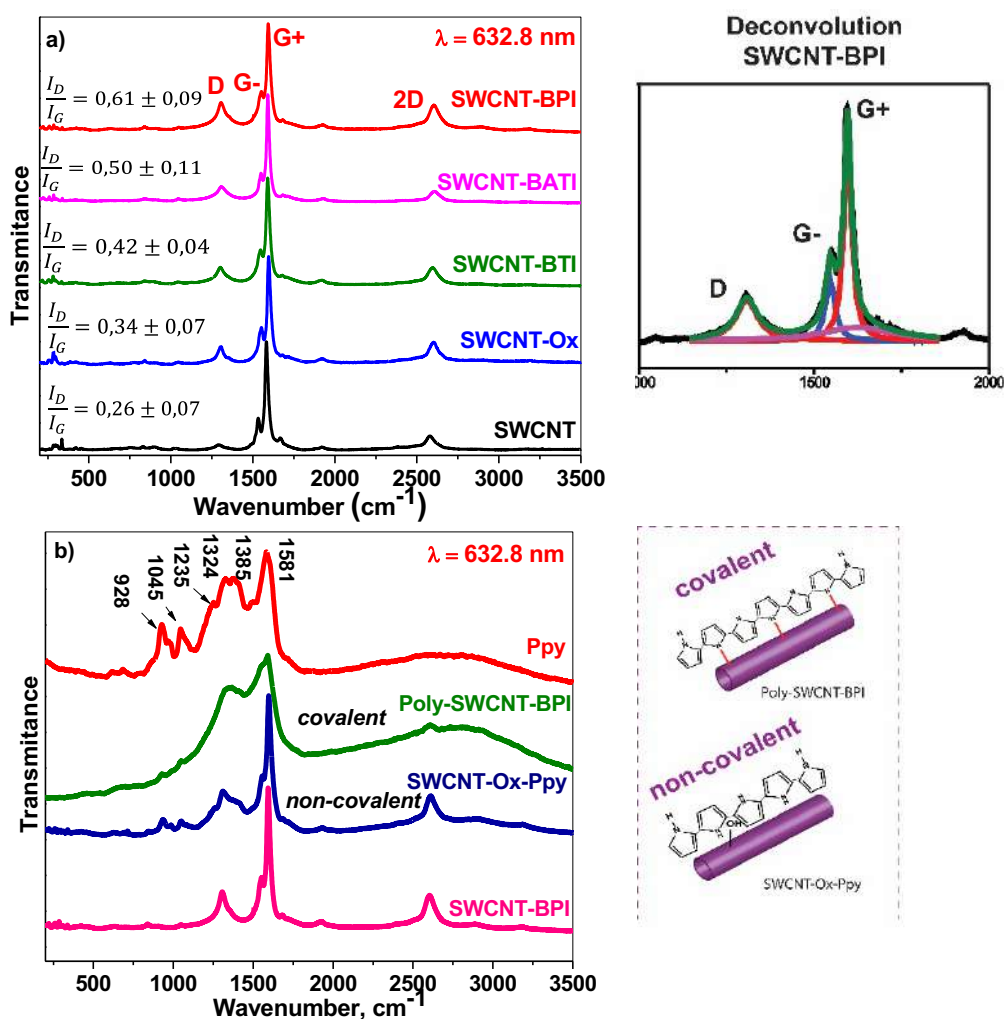


Figure 6. Representative Raman spectra (a) of the samples with excitation at 632.8 nm, showing the I_D/I_G value increases from SWCNT<SWCNT-Ox<SWCNT-BTI<SWCNT-BATI<SWCNT-BPI; the inset shows a representative SWCNT-BPI Raman deconvolution. Also are shown the representative Raman spectra (b) of the covalent and non-covalent nanocomposites.

Table 2. Raman bands of Ppy.[46-48]

Band position (cm^{-1})	
1581	C=C stretching (carbon skeleton)
1385	antisymmetric C-N stretching
1324	C-C stretching of the neutral species
1235	antisymmetric C-H (plane) bending
1080	C-H (plane) bending of oxidized species
1045	C-H (plane) bending of neutral species
970	cationic ring deformation of Ppy
928	ring deformation associated to dication

Additionally, FTIR analysis (spectra on Figure 7) shows significant differences when comparing the functionalized samples and raw SWCNTs. For raw SWCNTs, the band at 1640 cm^{-1} is due to the vibrational modes of C=C and the band at 3450 cm^{-1} is due to O-H groups that can be related to atmospheric moisture attached to SWCNTs.[49, 50] Similar features are observed on the SWCNT-Ox spectra. The formation of new bands in the spectra *e.g.* at 1200 cm^{-1} , 1730 cm^{-1} (C=O) for SWCNT-BATI and 1431 cm^{-1} for SWCNT-BPI and 1030 cm^{-1} for both, indicates functionalization. The band at 1431 cm^{-1} in the SWCNT-BPI spectra may be attributed to the stretching of C-N from pyrrole ring [51, 52] and at 1030 cm^{-1} to C-N stretching related to the amine groups [35]. Upon polymerization, FTIR analysis of Poly-SWCNT-BPI and SWCNT-Ox-Ppy shows the typical bands of Ppy.[48] Focus is given to the presence of the band at 960 cm^{-1} attributed to the C-C out-of-plane vibrations. This is a characteristic signature of Ppy polymerization. Overall, the FTIR analysis provides additional evidence of SWCNT functionalization and successful polymerization of the nanocomposites.

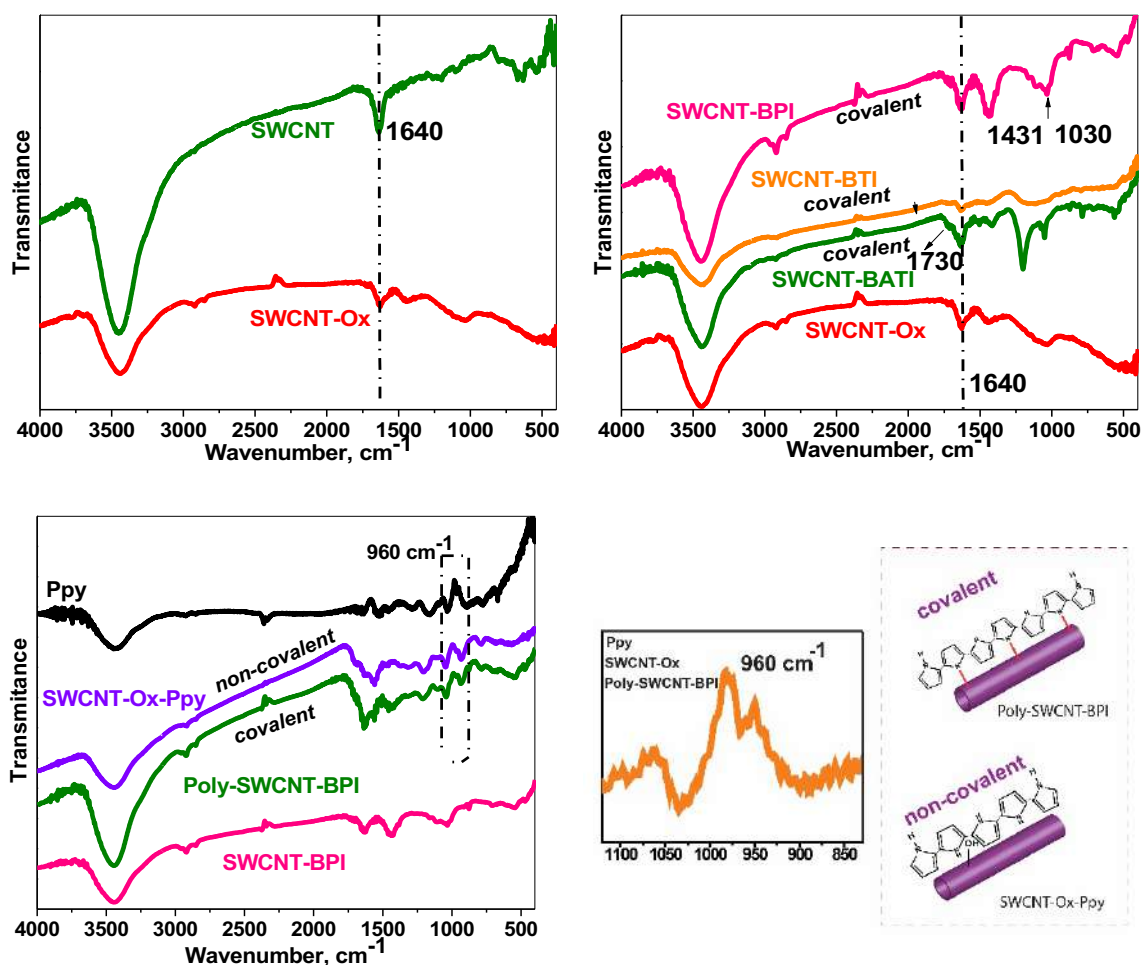


Figure 7. FTIR transmission spectra of functionalized samples (SWCNT-Ox, SWCNT-BATI, SWCNT-BTI) and the covalently and non-covalently linked nanocomposites (Poly-SWCNT-BPI and SWCNT-Ox-Ppy).

Figure 8 presents the TGA data of the functionalized SWCNTs (SWCNT-BPI, SWCNT-BATI e SWCNT-BTI). Differences can be observed on the shape of the TGA curves. The raw SWCNT sample presents two weight loss events: at 418 °C ascribed to the decomposition of carbon skeleton and at 721 °C related to the remaining catalyst (Mo).[53] The SWCNT-Ox sample presents only one weight loss, related to the decomposition of carbon skeleton, indicating the absence of catalyst in this sample, as expected due to the preparation methodology.

The SWCNT-BATI sample also presents two weight loss events, the first one at 176 °C associated with evaporation of the remaining solvent (DMSO) and the second at

432 °C, ascribed to the decomposition of functionalized groups on the surface of SWCNTs and to the carbon skeleton. Regarding to the other functionalized SWCNTs, these present only one weight loss (430 °C to SWCNT-BTI and 445 °C to SWCNT-BPI) related to the functionalized groups on the surface of the SWCNTs and to the carbon skeleton. In this case, no additional mass loss can be depicted, which is also expected for low degrees of functionalization.[9] The main differences between the TGA curves is related to the small and continuous weight loss starting at 100°C. The raw SWCNT presents a TGA curve with a flat curvature in the range of 100 – 320°C, whereas the functionalized samples present a continuous weight of loss starting in 100°C, presenting an intense sloping curvature until the end of decomposition. This means that there is a decrease on the thermal stability after the functionalization, as shown previously in the literature. [9, 54]

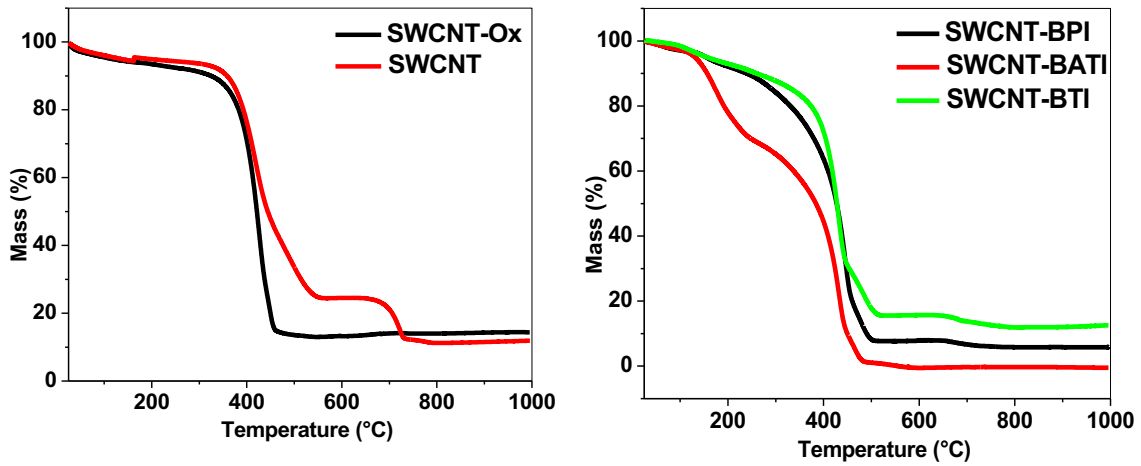


Figure 8. TGA of the samples of the raw and functionalized SWCNTs in air.

SEM images, Figure 9, show the morphology of the raw and functionalized SWCNTs. The samples are mainly composed of aggregates of tubular structures of CNT before and after the functionalization. The process of functionalization does not

alter the characteristic SWCNTs morphology. The morphology of the covalently linked nanocomposite are compared to the non-covalently linked nanocomposite (Figure 9). The structures are aggregated into bundles showing the polymer wrapping the tubes in Poly-SWCNT-BPI. No free SWCNT-BPI is visible and, from the observed morphology, we assume that the SWCNT-BPI are coated by the polymer. Evaluating the non-covalent nanocomposite, SWCNT-Ox-Ppy, two main regions are observed: one containing the globular structure of Ppy (circled blue lines) and the other containing the SWCNT-Ox coated with Ppy (circled red lines)[55]. The stronger interactions in the covalent nanocomposite in contrast to the non-covalent may induce the morphological differences observed.

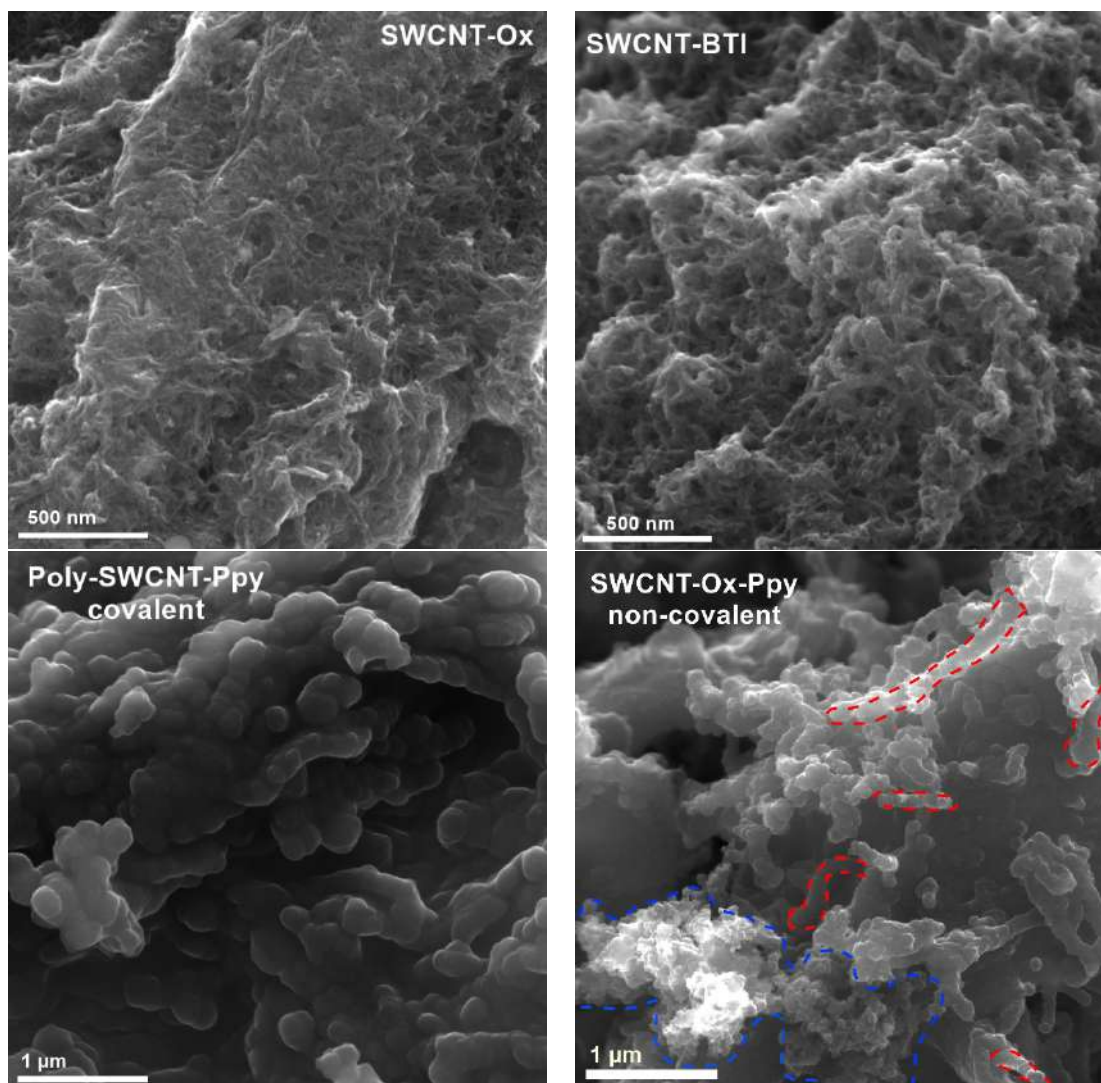


Figure 9. SEM images of the oxidized and functionalized SWCNTs, covalent and non-covalent linked nanocomposite.

As widely discussed in the literature [56-58] covalent functionalization of carbon nanomaterials nowadays continue to be a challenge, despite their many promising applications. Pursuing novel routes or improvements of known methodologies is thus important. Overall, in this paper we have synthesized and characterized three different SWCNT functionalized materials, covalently attached on the carbon skeleton structure of SWCNT with different monomers, employing mild reaction conditions. Moreover, the functionalized material was susceptible of polymerization, resulting in a nanocomposite of SWCNT with a covalently attached polymer. As a proof of concept, we pursued the polymerization of the pyrrole-derived material and the functionalized SWCNT yielded a polymeric nanocomposite for which we expect a synergistic effect between SWCNTs and polypyrrole. Regarding the polymerization process, we believe that the monomers anchored on the surface of SWCNTs take part in the process of chemical oxidative polymerization, providing a polymer anchored on the surface of the SWCNT (Figure 10).[48]. Likewise, the polymer formed is comprised of monomers freely available (pyrrole from the reaction medium) and also the pyrrole derivative attached to the CNT, leading to a highly interconnected polymer, strongly linked to the CNT. Thereby, the polymer is wrapping the SWCNT-BPI through a covalent bond providing a homogeneous morphology. In contrast, for the non-covalent nanocomposites, polymer wrapping is not homogeneously distributed and regions containing only Ppy are observed.

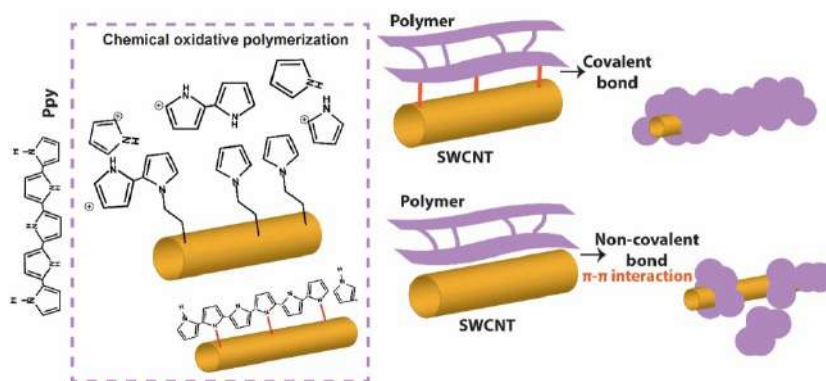


Figure 10. Schematic representation of the reaction mechanism and covalently and non-covalently final nanocomposites.

4. Conclusions

The complexity of organic chemistry reactions on carbon structures limits the carbon functionalization, nowadays presented as a strategic tool for development of new materials with promising applications. Herein, we have functionalized SWCNTs with three different monomers by a one-step and room temperature reaction. Also, we have synthesized covalent and non-covalent nanocomposites of SWCNT and Ppy, the former based on a covalently anchored monomer polymerization forming nanocomposites of conductive polymer on the carbon skeleton of the SWCNT and the latter based on π - π interactions. The covalent attachment of the monomers on the surface of SWCNT was confirmed by XPS measurements, Raman spectroscopy, and other techniques. Regarding the covalent and non-covalent polymerized nanocomposites, both presented similar chemical properties and, in both composites, the Ppy was in the conductive form. Nevertheless, SEM images show a more homogeneous coverage of SWCNTs with Ppy on the covalently linked nanocomposite (Poly-SWCNT-BPI). Overall, the challenge of carbon functionalization has been successfully accomplished. The development of different routes to obtain new materials, *e.g.* decreasing the number of reactions steps and favoring mild conditions,

is an advance in the functionalization chemistry of carbon structures. In this paper, using a one-step reaction under mild conditions, the CNT functionalization has been simplified. The strategy adopted here allows the functionalization of CNTs with several other molecules and potentiates new application possibilities of CNT nanocomposites.

5. References

- [1] F.V. Ferreira, W. Francisco, B.R.C.d. Menezes, L.D.S. Cividanes, A.d.R. Coutinho, G.P. Thim, Carbon nanotube functionalized with dodecylamine for the effective dispersion in solvents, *Applied Surface Science* 357, Part B (2015) 2154-2159.
- [2] A. Pénicaud, P. Poulin, A. Derré, E. Anglaret, P. Petit, Spontaneous Dissolution of a Single-Wall Carbon Nanotube Salt, *Journal of the American Chemical Society* 127(1) (2005) 8-9.
- [3] D. Tasis, N. Tagmatarchis, A. Bianco, M. Prato, Chemistry of Carbon Nanotubes, *Chemical Reviews* 106(3) (2006) 1105-1136.
- [4] S. Husmann, A.J.G. Zarbin, Design of a Prussian Blue Analogue/Carbon Nanotube Thin-Film Nanocomposite: Tailored Precursor Preparation, Synthesis, Characterization, and Application, *Chemistry – A European Journal* 22(19) (2016) 6643-6653.
- [5] M.C. Schnitzler, M.M. Oliveira, D. Ugarte, A.J.G. Zarbin, One-step route to iron oxide-filled carbon nanotubes and bucky-onions based on the pyrolysis of organometallic precursors, *Chemical Physics Letters* 381(5) (2003) 541-548.
- [6] P. Bilalis, D. Katsigiannopoulos, A. Avgeropoulos, G. Sakellariou, Non-covalent functionalization of carbon nanotubes with polymers, *RSC Advances* 4(6) (2014) 2911-2934.
- [7] L. Vaisman, H.D. Wagner, G. Marom, The role of surfactants in dispersion of carbon nanotubes, *Advances in Colloid and Interface Science* 128-130 (2006) 37-46.
- [8] S. Yaragalla, G. Anilkumar, N. Kalarikkal, S. Thomas, Structural and optical properties of functionalized multi-walled carbon nanotubes, *Materials Science in Semiconductor Processing* 41 (2016) 491-496.
- [9] D. Voiry, O. Roubeau, A. Penicaud, Stoichiometric control of single walled carbon nanotubes functionalization, *Journal of Materials Chemistry* 20(21) (2010) 4385-4391.
- [10] Z. Spitalsky, D. Tasis, K. Papagelis, C. Galiotis, Carbon nanotube–polymer composites: Chemistry, processing, mechanical and electrical properties, *Progress in Polymer Science* 35(3) (2010) 357-401.
- [11] Y. Qiu, X. Wang, H. Huang, Z. Cheng, X. Chang, L. Guo, Ferrocenyl-functionalized carbon nanotubes with greatly improved surface reactivity for enhancing electrocapacitance, *Journal of Organometallic Chemistry* 880 (2019) 349-354.
- [12] K.M. Lee, C.P.P. Wong, T.L. Tan, C.W. Lai, Functionalized carbon nanotubes for adsorptive removal of water pollutants, *Materials Science and Engineering: B* 236-237 (2018) 61-69.
- [13] M. Manoj, C. Muhamed Ashraf, M. Jasna, K.M. Anilkumar, B. Jinisha, V.S. Pradeep, S. Jayalekshmi, Biomass-derived, activated carbon-sulfur composite cathode with a bifunctional interlayer of functionalized carbon nanotubes for lithium-sulfur cells, *Journal of Colloid and Interface Science* 535 (2019) 287-299.
- [14] G.A.M. Ali, E.Y. Lih Teo, E.A.A. Aboelazm, H. Sadegh, A.O.H. Memar, R. Shahryari-Ghoshekandi, K.F. Chong, Capacitive performance of cysteamine functionalized carbon nanotubes, *Materials Chemistry and Physics* 197 (2017) 100-104.

- [15] M. Habibizadeh, K. Rostamizadeh, N. Dalali, A. Ramazani, Preparation and characterization of PEGylated multiwall carbon nanotubes as covalently conjugated and non-covalent drug carrier: A comparative study, *Materials Science and Engineering: C* 74 (2017) 1-9.
- [16] M. Adamska, U. Narkiewicz, Fluorination of Carbon Nanotubes – A Review, *Journal of Fluorine Chemistry* 200 (2017) 179-189.
- [17] W. Zhang, K. Guérin, M. Dubois, Z.E. Fawal, D.A. Ivanov, L. Vidal, A. Hamwi, Carbon nanofibres fluorinated using TbF₄ as fluorinating agent. Part I: Structural properties, *Carbon* 46(7) (2008) 1010-1016.
- [18] B.N. Khare, M. Meyyappan, A.M. Cassell, C.V. Nguyen, J. Han, Functionalization of Carbon Nanotubes Using Atomic Hydrogen from a Glow Discharge, *Nano Letters* 2(1) (2002) 73-77.
- [19] Y. Xu, X. Wang, R. Tian, S. Li, L. Wan, M. Li, H. You, Q. Li, S. Wang, Microwave-induced electrophilic addition of single-walled carbon nanotubes with alkylhalides, *Applied Surface Science* 254(8) (2008) 2431-2435.
- [20] M.S. Polyakov, T.V. Basova, M. Göksel, A. Şenocak, E. Demirbaş, M. Durmuş, B. Kadem, A. Hassan, Effect of covalent and non-covalent linking of zinc(II) phthalocyanine functionalised carbon nanomaterials on the sensor response to ammonia, *Synthetic Metals* 227 (2017) 78-86.
- [21] B. Kadem, M. Göksel, A. Şenocak, E. Demirbaş, D. Atilla, M. Durmuş, T. Basova, K. Shanmugasundaram, A. Hassan, Effect of covalent and non-covalent linking on the structure, optical and electrical properties of novel zinc(II) phthalocyanine functionalized carbon nanomaterials, *Polyhedron* 110 (2016) 37-45.
- [22] J. Mao, Y. Wang, J. Zhu, J. Yu, Z. Hu, Thiol functionalized carbon nanotubes: Synthesis by sulfur chemistry and their multi-purpose applications, *Applied Surface Science* 447 (2018) 235-243.
- [23] Z. Yao, N. Braid, G.A. Botton, A. Adronov, Polymerization from the Surface of Single-Walled Carbon Nanotubes – Preparation and Characterization of Nanocomposites, *Journal of the American Chemical Society* 125(51) (2003) 16015-16024.
- [24] J. Cui, W. Wang, Y. You, C. Liu, P. Wang, Functionalization of multiwalled carbon nanotubes by reversible addition fragmentation chain-transfer polymerization, *Polymer* 45(26) (2004) 8717-8721.
- [25] F. Hof, S. Bosch, S. Eigler, F. Hauke, A. Hirsch, New Basic Insight into Reductive Functionalization Sequences of Single Walled Carbon Nanotubes (SWCNTs), *Journal of the American Chemical Society* 135(49) (2013) 18385-18395.
- [26] D. Voiry, C. Drummond, A. Penicaud, Portrait of carbon nanotube salts as soluble polyelectrolytes, *Soft Matter* 7(18) (2011) 7998-8001.
- [27] A. Catheline, C. Valles, C. Drummond, L. Ortolani, V. Morandi, M. Marcaccio, M. Iurlo, F. Paolucci, A. Penicaud, Graphene solutions, *Chemical Communications* 47(19) (2011) 5470-5472.
- [28] A. Pénicau, C. Drummond, Deconstructing Graphite: Graphenide Solutions, *Accounts of Chemical Research* 46(1) (2013) 129-137.
- [29] A. Pénicau, F. Dragin, G. Pécastaings, M. He, E. Anglaret, Concentrated solutions of individualized single walled carbon nanotubes, *Carbon* 67 (2014) 360-367.
- [30] D. Voiry, C. Vallés, O. Roubéau, A. Pénicau, Dissolution and alkylation of industrially produced multi-walled carbon nanotubes, *Carbon* 49(1) (2011) 170-175.
- [31] G. Bepete, N. Izard, F. Torres-Canas, A. Derré, A. Sbardelotto, E. Anglaret, A. Pénicau, C. Drummond, Hydroxide Ions Stabilize Open Carbon Nanotubes in Degassed Water, *ACS Nano* 12(8) (2018) 8606-8615.
- [32] G. Bepete, F. Hof, K. Huang, K. Kampioti, E. Anglaret, C. Drummond, A. Pénicau, "Eau de graphene" from a KC8 graphite intercalation compound prepared by a simple mixing of graphite and molten potassium, *physica status solidi (RRL) – Rapid Research Letters* 10(12) (2016) 895-899.

- [33] R.A. Schäfer, J.M. Englert, P. Wehrfritz, W. Bauer, F. Hauke, T. Seyller, A. Hirsch, On the Way to Graphane—Pronounced Fluorescence of Polyhydrogenated Graphene, *Angewandte Chemie International Edition* 52(2) (2013) 754-757.
- [34] D. Voiry, O. Roubeau, A. Pénicaud, Stoichiometric control of single walled carbon nanotubes functionalization, *Journal of Materials Chemistry* 20(21) (2010) 4385.
- [35] M. Gholami, P.M. Nia, Y. Alias, Morphology and electrical properties of electrochemically synthesized pyrrole–formyl pyrrole copolymer, *Applied Surface Science* 357, Part A (2015) 806-813.
- [36] M. Varga, T. Izak, V. Vretenar, H. Kozak, J. Holovsky, A. Artemenko, M. Hulman, V. Skakalova, D.S. Lee, A. Kromka, Diamond/carbon nanotube composites: Raman, FTIR and XPS spectroscopic studies, *Carbon* 111 (2017) 54-61.
- [37] S. Ratso, I. Kruusenberg, A. Sarapuu, P. Rauwel, R. Saar, U. Joost, J. Aruväli, P. Kanninen, T. Kallio, K. Tammeveski, Enhanced oxygen reduction reaction activity of iron-containing nitrogen-doped carbon nanotubes for alkaline direct methanol fuel cell application, *Journal of Power Sources* 332 (2016) 129-138.
- [38] T. Ji, L. Chen, L. Mu, R. Yuan, M. Knoblauch, F.S. Bao, J. Zhu, In-situ reduction of Ag nanoparticles on oxygenated mesoporous carbon fabric: Exceptional catalyst for nitroaromatics reduction, *Applied Catalysis B: Environmental* 182 (2016) 306-315.
- [39] Y.-j. Tao, Y.-j. Zhou, X.-q. Xu, Z.-y. Zhang, H.-f. Cheng, W.-w. Zheng, A multielectrochromic copolymer based on anthracene and thiophene via electrochemical copolymerization in boron trifluoride diethyl etherate, *Electrochimica Acta* 78 (2012) 353-358.
- [40] J. Kettle, Z. Ding, M. Horie, G.C. Smith, XPS analysis of the chemical degradation of PTB7 polymers for organic photovoltaics, *Organic Electronics* 39 (2016) 222-228.
- [41] L. Ruangchuay, J. Schwank, A. Sirivat, Surface degradation of α -naphthalene sulfonate-doped polypyrrole during XPS characterization, *Applied Surface Science* 199(1–4) (2002) 128-137.
- [42] J. Tabačiarová, M. Mičušík, P. Fedorko, M. Omastová, Study of polypyrrole aging by XPS, FTIR and conductivity measurements, *Polymer Degradation and Stability* 120 (2015) 392-401.
- [43] V.W.L. Lim, S. Li, E.T. Kang, K.G. Neoh, K.L. Tan, In situ XPS study of thermally deposited aluminium on chemically synthesized polypyrrole films, *Synthetic Metals* 106(1) (1999) 1-11.
- [44] M.S. Dresselhaus, G. Dresselhaus, R. Saito, A. Jorio, Raman spectroscopy of carbon nanotubes, *Physics Reports* 409(2) (2005) 47-99.
- [45] L. Hostert, S.F. Blaskiewicz, J.E.S. Fonsaca, S.H. Domingues, A.J.G. Zarbin, E.S. Orth, Imidazole-derived graphene nanocatalysts for organophosphate destruction: Powder and thin film heterogeneous reactions, *Journal of Catalysis* 356 (2017) 75-84.
- [46] K. Crowley, J. Cassidy, In situ resonance Raman spectroelectrochemistry of polypyrrole doped with dodecylbenzenesulfonate, *Journal of Electroanalytical Chemistry* 547(1) (2003) 75-82.
- [47] X. Zuo, Y. Zhang, L. Si, B. Zhou, B. Zhao, L. Zhu, X. Jiang, One-step electrochemical preparation of sulfonated graphene/polypyrrole composite and its application to supercapacitor, *Journal of Alloys and Compounds* 688, Part B (2016) 140-148.
- [48] N. Naidek, A.J.G. Zarbin, E.S. Orth, Covalently linked nanocomposites of polypyrrole with graphene: Strategic design toward optimized properties, *Journal of Polymer Science Part A: Polymer Chemistry* 56(6) (2018) 579-588.
- [49] L. Chen, H. Zhou, C. Fu, Z. Chen, C. Xu, Y. Kuang, Chemical modification of pristine carbon nanotubes and their exploitation as the carbon hosts for lithium-sulfur batteries, *International Journal of Hydrogen Energy* 41(47) (2016) 21850-21860.
- [50] R.S. Chouhan, A. Qureshi, B. Yagci, M.A. Gülgün, V. Ozguz, J.H. Niazi, Biotransformation of multi-walled carbon nanotubes mediated by nanomaterial resistant soil bacteria, *Chemical Engineering Journal* 298 (2016) 1-9.

- [51] S. Idris, A.A. A. Bakar, C. Thevy Ratnam, N.H. Kamaruddin, S. Shaari, Influence of gamma irradiation on polymerization of pyrrole and glucose oxidase immobilization onto poly (pyrrole)/poly (vinyl alcohol) matrix, *Applied Surface Science* 400 (2017) 118-128.
- [52] M.B.G. Costa, J.M. Juárez, M.L. Martínez, A.R. Beltramone, J. Cussa, O.A. Anunziata, Synthesis and characterization of conducting polypyrrole/SBA-3 and polypyrrole/Na–AISBA-3 composites, *Materials Research Bulletin* 48(2) (2013) 661-667.
- [53] S. Rajagopal, D. Nataraj, O.Y. Khyzhun, Y. Djaoued, J. Robichaud, K. Senthil, D. Mangalaraj, Systematic synthesis and analysis of change in morphology, electronic structure and photoluminescence properties of pyrazine intercalated MoO₃ hybrid nanostructures, *CrystEngComm* 13(7) (2011) 2358-2368.
- [54] R.A. Moraes, C.F. Matos, E.G. Castro, W.H. Schreiner, M.M. Oliveira, A.J.G. Zabin, The effect of different chemical treatments on the structure and stability of aqueous dispersion of iron- and iron oxide-filled multi-walled carbon nanotubes, *Journal of the Brazilian Chemical Society* 22 (2011) 2191-2201.
- [55] H. Song, K. Cai, J. Wang, S. Shen, Influence of polymerization method on the thermoelectric properties of multi-walled carbon nanotubes/polypyrrole composites, *Synthetic Metals* 211 (2016) 58-65.
- [56] A. Kasprzak, A. Zuchowska, M. Poplawska, Functionalization of graphene: does the organic chemistry matter?, *Beilstein Journal of Organic Chemistry* 14 (2018) 2018-2026.
- [57] M. Schirowski, G. Abellán, E. Nuin, J. Pampel, C. Dolle, V. Wedler, T.-P. Fellingner, E. Spiecker, F. Hauke, A. Hirsch, Fundamental Insights into the Reductive Covalent Cross-Linking of Single-Walled Carbon Nanotubes, *Journal of the American Chemical Society* 140(9) (2018) 3352-3360.
- [58] G. Bottari, M.Á. Herranz, L. Wibmer, M. Volland, L. Rodríguez-Pérez, D.M. Guldi, A. Hirsch, N. Martín, F. D'Souza, T. Torres, Chemical functionalization and characterization of graphene-based materials, *Chemical Society Reviews* 46(15) (2017) 4464-4500.